



DR DAVID SABATINO (Orcid ID : 0000-0002-9797-0833)

Article type : Special Issue Article

Solid Phase Synthesis and Self-Assembly of Higher-Order siRNAs and their Bioconjugates

Christopher N. Cultrara¹, Sunil Shah¹, Stephen D. Kozuch¹, Mayurbhai R. Patel² and David Sabatino^{1,*}

¹Department of Chemistry and Biochemistry, Seton Hall University, South Orange, NJ 07079

²Nitto Denko AVECIA Inc, 8560 Reading Road, Cincinnati, OH 45215

*Corresponding Author: David Sabatino: Email ID : david.sabatino@shu.edu

Tel : +1-973-313-6359

Abstract

New methods for the synthesis of higher-order siRNA motifs and their bioconjugates have recently gained widespread attention in the development of new and improved gene therapeutics. Our efforts aim to produce new chemical tools and protocols for the generation of modified siRNAs that This article has been accepted for publication and undergone full peer review but has not been through the copyediting, typesetting, pagination and proofreading process, which may lead to differences between this version and the Version of Record. Please cite this article as doi: 10.1111/cbdd.13448

This article is protected by copyright. All rights reserved.

Accepted Article

screen for important oncogene targets as well as silence their activity for effective gene therapy in cancer models. More specifically, we have developed an efficient solution-phase synthesis for the production of a ribouridine branchpoint synthon that can be effectively incorporated by solid phase synthesis within higher-order RNA structures, including those adopting V-, and Y- and >-< shape RNA templates. Self-assembly of complementary RNA to the template strands produced higher-order siRNA nanostructures that were characterized by a combination of PAGE, DLS and TEM techniques. In an effort to extend the repertoire of functionally diverse siRNAs, we have also developed solid phase bioconjugation strategies for incorporating bio-active probes such as fatty acid appendages and fluorescent reporters. Taken together, these methods highlight the ability to generate higher-order siRNAs and their bioconjugates for exploring the influence of modified siRNA structure on anti-cancer activity.

INTRODUCTION

Among the many nucleic acids currently employed as gene therapy agents, short-interfering RNAs (siRNAs) are widely used as potent regulators of gene expression and for mitigating the progression of various diseases.¹⁻³ Structurally, siRNAs are short double stranded RNA duplexes composed of hybrid antisense (guide) and sense (passenger) strands which contain 19-25 base pairs with nucleotide overhangs on the 3' ends.⁴⁻⁶ These molecules have the ability to activate the RNA interference (RNAi) pathway, which is a naturally occurring regulatory mechanism of gene translation. In this mechanism, long double stranded RNAs are cleaved into siRNAs by an RNase III dependent endonuclease referred to as "Dicer". The siRNA are then incorporated into the RNA Induced Silencing Complex (RISC), a multimeric protein complex with endonuclease activity mediated by the Argonaute (Ago) protein which uses the guide strand to target and cleave complementary mRNA, thus preventing protein translation.⁷⁻¹⁰

In spite of their therapeutic promise, siRNAs are still plagued by poor pharmacokinetic properties,¹¹ including poor metabolic stability, off-target gene silencing and immunostimulatory effects which raises toxicity, limited cell permeability and duration of action which restricts their therapeutic potential and raises the need for more potent constructs. One approach to improve siRNA potency is to combine multiple siRNAs which target a single or multiple mRNA target sequences. However, effectively delivering or expressing multiple siRNAs in a cell has proven to be difficult, with limited *in vivo* applicability.¹² Alternatively, chemically derived siRNAs can facilitate the incorporation of modifications or functional probes which can enable self-assembly into higher-order structures for improving RNAi activity.¹³⁻¹⁵

RNAi nanotechnology has led to the evolution of functional siRNA materials for a variety of applications, including the development of nanomedicines and nanoparticle formulations for gene therapy.^{14,15} siRNA nanostructures have been formulated for silencing single or multiple gene targets. For example, a tripodal-interfering RNA (tiRNA) (Figure 1, a) and related supramolecular RNA nanostructures with polyethyleneimine (PEI) and galactose-functionalized PEI were self-assembled to promote silencing efficiency *in-vivo*.¹³ These combination approaches produced siRNA nanoparticle formulations which improved siRNA stability, cell permeability and accumulation into the liver for a more potent and long-lasting mRNA knockdown effect relative to the linear siRNA controls. Furthermore, DNA-RNA and RNA-RNA nanocubes (Figure 1, b), the latter of which contained as many as six double-stranded dsRNA Dicer substrates, promoted the release of multiple siRNAs in breast cancer cells.¹⁶ The siRNAs resulted in enhanced green fluorescent protein, (eGFP) knockdown for up to twelve (12) days. Moreover, in functional studies, the RNA nanocubes induced potent suppression of the viral Gag proteins, p55 and p24, in HIV-1 pseudotyped with VSV-g 293T cells, which resulted in potent antiviral activity. However, these constructs were also found to be immunogenic, thereby limiting their therapeutic utility and raising toxicity concerns. In another proof-of-concept study, the siRNA nanostructures composed of self-assembled three- and four-way junctions (Figure 1, c), triggered potent knockdown of multiple luciferase gene targets for up to five (5) days in HeLa cells.¹⁷

These representative examples highlight the potential utility of siRNA nanostructures in therapeutic RNAi applications.

Figure 1. Schematic representations of siRNA self-assembly and nanotechnology.

Building on this work, we have developed novel “branched” V- and Y-shape RNA scaffolds on solid phase that respectively facilitated the self-assembly of two (2) and three (3) (Figure 1, d) siRNA sequences silencing a single or multiple mRNA targets. Initially, the higher order V- and Y-shape siRNAs targeted multiple mRNA sites belonging to GRP78, a master regulator of the unfolded protein response (UPR) and endoplasmic reticulum (ER) stress pathways that are overexpressed in cancerous tissues and related to cancer cell survival and tumor progression. The resultant V-shape (2 siRNAs) and Y-shape (3 siRNAs) were found to be more active than a linear siRNA control which silenced a single GRP78 mRNA site. The V- and Y-shape siRNAs led to notable gene knockdown (50-60%) and toxicity (5-15%) in HepG2 liver cancer cells.¹⁸

In an attempt to further improve knockdown efficiency of multiple Glucose Regulated Proteins (GRPs), the V- and Y-shape RNA templates were self-assembled with complementary RNA resulting in the siRNA hybrids against the resident oncogenic GRPs (GRP78, GRP94 and GRP75). siRNA self-assembly formed a wide variety of nanostructures (50-100 nm), of which a lead Y-shape siRNA targeting GRP78, GRP94, and GRP75 elicited >80 % gene silencing for up to 72 hours. This synergistic GRP knockdown effect translated into 50% cell death in an endometrial (AN3CA) cancer cell line. Its activity was found to be comparable in other cancer cell lines related to the cervix (HeLa) and breast (MDA-MB-231) that overexpressed GRP. However, when compared to a non-tumorigenic lung (MRC5) cell line which displayed normal GRP levels, a reduced knockdown effect was observed within this control cell line. This observation may relate to siRNA treatment specificity in cancer cell lines which overexpress GRP activity. Moreover, the Y-shape siRNA nanostructure targeting all three (3)

oncogenic GRPs produced a 5-fold increase in cytotoxicity in cancer cells compared to the linear siRNA control, underscoring its utility in oncogene therapy applications.¹⁹

siRNA bioconjugates have shown the potential to improve the physicochemical and pharmacokinetic properties of siRNAs in preclinical and clinical studies.²⁰⁻²² Among these modifications, the incorporation of lipid appendages such as fatty acids, terpenes and steroids (Figure 2, a) have been widely used for generating amphiphilic siRNA bioconjugates that have improved metabolic stability, enhanced cell permeability and promoted longer duration of action when compared to the control, unconjugated siRNAs.²³⁻²⁶ Moreover, the integration of therapy and diagnostics termed “theranostics” has led to the development of new and improved gene therapeutics for the diagnosis and treatment of cancers.²⁷ Specifically, siRNA bioconjugates containing reporter probes such as fluorophores, near-infrared (near IR) dyes and photosensitizers as well as those containing contrast agents and radiolabels (Figure 2, b) have been extensively applied as theranostic agents in oncology.^{28,29}

In spite of the many fruitful examples of siRNA bioconjugation and their applications in cancer gene therapy, a major limitation is the restriction of a single functional moiety on either the 3' or 5' ends of the oligonucleotide. In order to address this limitation, our methodology using the V- and Y-shape RNA templates, facilitated the incorporation of multiple reporter, fluorescein isothiocyanate (FITC) or fatty acid groups within a single siRNA scaffold belonging to either the linear, V-shape or Y-branch siRNA motifs (Figure 2, c, d).^{30,31} Increasing FITC labeling improved fluorescent signaling and imaging within prostate cancer (PC-3) cells while retaining GRP knockdown and cell death efficacy.³⁰ Furthermore, the multiple fatty acid groups enabled some PC-3 cells' uptake of the siRNA in the absence of a transfection reagent. The fatty acid conjugated siRNAs also improved serum stability which resulted in notable GRP mRNA knockdown when compared to the native siRNA control.³¹

Figure 2. Representative examples of siRNA bioconjugates.

Taken together, these representative examples demonstrate the fruitful applications of our solid phase RNA synthesis methodology. This method is useful for the incorporation of a unique branchpoint synthon that can produce multiple higher-order V- and Y-shape RNA templates. These templates can facilitate self-assembly with complementary RNA to generate higher-order siRNA nanostructures (Figure 1, d) and bioconjugates (Figure 2, c, d) useful for potentiating RNAi activity in cancer cells. The synthetic protocols associated with the preparation of these novel siRNA motifs are described.

RESULTS AND DISCUSSION

Higher-order siRNA Nanostructure Formulations

In the generation of newly modified siRNA structures, we initially developed a 4 step solution phase synthesis procedure for the development of an orthogonally protected branchpoint ribouridine phosphoramidite (Scheme 1).¹⁸ In our synthesis method, levulinic acid was initially converted into the anhydride and used to esterify selectively the 5'-OH group of ribouridine following a chemoenzymatic reaction using a support-bound lipase, Novozyme, as the catalytic component.¹⁸ The reaction produced a single product as detected by TLC and isolated following sample filtration and concentration *in vacuo*. The sample purity and identity of 5'-levulinyl ribouridine, **2**, was confirmed by a combination of ¹H, ¹³C NMR and MS.¹⁸ The 5'-levulinyl ribouridine, **2**, was then tritylated to the 5'-levulinyl 2' and 3' -MMT ribouridine regioisomers, **3** and **4**, respectively, that were separable by column chromatography and characterized by NMR and MS. NMR COSY crosspeaks were used to identify the regioisomers by correlating the 2'H with the 2'OH for the 3'-MMT isomer, **4**, and the 3'H with the 3'OH for the 2'MMT isomer, **3**. The isolated 5'-levulinyl 2'-MMT ribouridine, **3**, was finally phosphitylated to the 3'-phosphoramidite diastereomers, **5**. The isolated diastereomers, **5**, were confirmed by ³¹P NMR and directly used as branchpoint synthon for the generation of V-, Y- and >-< shape siRNA.¹⁸

Scheme 1. Solution-phase synthesis of the ribouridine branchpoint phosphoramidites, **5**.

The synthesis strategy for constructing our 1st generation higher-order siRNA structures on solid phase was initiated with linear RNA synthesis (1 μ mol) on a long chain alkyl amino (LCAA) functionalized controlled pore glass (CPG) solid support. Following RNA synthesis, the incorporation of the orthogonally protected branchpoint phosphoramidite, **5**, was added at the 5'-end of the linear RNA strand followed by an extended (15 min) coupling time using ethylthiotetrazole (ETT) as activator and coupling reagent. Decyanoethylation was subsequently completed with 4:6 v/v triethylamine in acetonitrile (NEt₃:MeCN) for 90 minutes. Removal of the phosphorous cyanoethyl protect groups was used to convert the reactive RNA phosphite triester into the more stable phosphite diester to avoid isomerization and degradation during the acidic conditions (3% DCA:DCM for 3 min) used for MMT removal.¹⁸ Following detritylation and liberation of the branchpoint 2'OH group, a second RNA synthesis was continued to generate the V-shape RNA on solid support (Scheme 2). Capping of the 5'end with acetic anhydride (Ac₂O) enabled selective delevulation (0.5M NH₂NH₂.H₂O in 3:2 v/v pyridine:acetic acid for 20 min) and extension of a third RNA segment from the branchpoint 5'OH group produced the Y-shape RNA template (Scheme 2). Repeating this cycle with the addition of a second branchpoint phosphoramidite afforded the >< shape RNA template (Scheme 2). Following solid phase synthesis, the RNA samples were cleaved and deprotected from the solid support using 3:1 v/v ammonium hydroxide: ethanol, NH₄OH:EtOH, and the 2'-OTBDMS groups were desilylated using 1:1.2 v/v trimethylamine trihydrofluoride:dimethylsulfoxide, TEA-3HF:DMSO, at 55 °C for 2 h. The crude RNA samples were precipitated in n-butanol (1 mL) and 3 M sodium acetate, NaOAc (25 μ L), centrifuged and isolated as a solid white pellet. RNA sample analyses and purifications were completed by Reverse Phase Ion Pairing High Performance Liquid Chromatography (RP IP HPLC), whereby sample identity was confirmed by molecular weight analyses using Electrospray Ionization Mass Spectrometry (ESI/MS) in negative mode. Pure RNA templates were hybridized into their corresponding linear, V-shape (RNA 1-2), Y-branch (RNA 1-2) and >< (RNA 1-2 and RNA 4-5) siRNAs in annealing buffer (10 mM Tris, 50 mM NaCl, 1 mM EDTA, pH 7.5–8.0, 13-15 μ L) for structure-activity relationship studies.¹⁸

Scheme 2. Solid phase synthesis of linear, V-, Y- and >-< shape RNA.

Inspired from our previous work which produced linear, V and Y shape RNA templates, we developed a self-assembly strategy for the generation of genetically encoded siRNA shapes (Figure 3). In our self-assembly approach, equimole (200 pmol) quantities of purified linear, V- and Y-shape RNA templates along with their complementary RNA strands were used to form the siRNA hybrids in annealing buffer (10 mM Tris, 50 mM NaCl, 1 mM EDTA, pH 7.5–8.0, 13-15 μ L). For the higher-ordered siRNA nanostructure formulations, each complementary RNA strand (linear, V or Y) was added to their corresponding RNA templates in stoichiometric ratios that favored hybrid formation. Self-assembly into siRNA nanostructures which mimicked the formation of circles, squares, rectangles, pentagons, hexagons and porous spheres that may be potentially useful in host-guest chemistry.³³ To promote hybridization and self-assembly of the siRNA nanostructure formulations, RNA templates (200 pmol) along with their complementary RNA strands (200 pmol) were heated at 90 °C (5-10 min) followed by slow cooling to room temperature (22 °C) for 1 h, and overnight storage at 4 °C prior to analysis. siRNA hybridization was confirmed by a native, non-denaturing 16% polyacrylamide gel electrophoresis (PAGE), followed by DLS studies and TEM imaging which confirmed the sizes and shapes of the higher-ordered siRNA nanostructures.¹⁹ Briefly, native PAGE analyses confirmed the formation of more retained, self-assembled higher-order siRNA hybrids, whereas TEM and DLS provided additional structural information related to the varying geometric shapes and sizes (10-150 nm) of the observed self-assembled siRNA nanostructures (Figure 3).

Figure 3. Design and self-assembly of siRNA nanostructures.

Solid phase RNA-fatty acid Bioconjugation

In this study, we have expanded the scope of lipidated siRNAs by incorporating various long chain fatty acids onto the 5' ends of the antisense and sense strands of the GRP-targeting linear, V- and Y-shape RNA templates. The siRNA sequences were based on the target nucleotides for down-regulating GRP-75, 78, and 94.¹⁸ Solid phase RNA synthesis of alkyl ((CH₂)₆) amino linker GRP78

This article is protected by copyright. All rights reserved.

antisense RNA (NH₂-(CH₂)₆-5'-AUC AGA AUC UUC CAA CAC U-3') and sense RNA (NH₂-(CH₂)₆-5'-AGU GUU GGA AGA UUC UGA U-3') were performed on a 2000Å UnyLinker CPG support (ChemGenes Inc.) using a 1 μmol scale automated synthesis cycle on a ABI 3400 synthesizer. A HCTU-coupling strategy was developed on solid-phase for the ligation of shorter and longer chain (C₁₂-C₁₈) fatty acids with saturated, unsaturated and polyunsaturated hydrocarbons onto the amino-linked linear RNA templates bound to the CPG solid supports (Scheme 3).³¹

Scheme 3. Solid-phase bioconjugation of the amino-linked linear, V and Y-shaped RNA templates with various fatty acids to afford the amide-linked fatty acid-RNA bioconjugates.

In our solid phase RNA bioconjugation approach, fatty acids were added to the resin bound RNA (0.1 μmol,) followed by the addition of a coupling reagent, O-(1H-6-chlorobenzotriazole-1-yl)-1,1,3,3-tetramethyluronium hexafluorophosphate, HCTU. The mixture was suspended in minimum DMF and a base, *N,N'*-diisopropylethylamine, DIEA, was added to initiate the reaction. Reactions were conducted in screw-cap Eppendorf microcentrifuge tubes and left overnight (16 h) at room temperature (22 °C) on a shaker. The CPG was subsequently washed three times with DMF/DCM/MeOH and dried *in vacuo*. The fatty acid conjugated to the resin bound RNA was cleaved and the RNA protecting groups removed using NH₄OH: EtOH (3:1 v/v) for 16 h at 55 °C. The crude RNA-fatty acid bioconjugates were evaporated to dryness, extracted in autoclaved water (1 mL), concentrated to dryness and re-suspended in a mixture of 1:1.5 v/v TEA-3HF:DMSO to complete the 2'-desilylation reaction at 65 °C for 2 h. The crude fatty acid RNA bioconjugates (Scheme 3, samples 1-10) were precipitated from the reaction mixture with 3 M NaOAc in n-BuOH at -80 °C (30 min) prior to centrifugation (~10,000 rpm, ~5 minutes) which left the crude samples as solid white pellets. The fatty acid RNA bioconjugates were then extracted into autoclaved water (1 mL), quantitated by UV-Vis spectrophotometry, analyzed and purified by RP IP HPLC on a Waters 2695 Alliance system.

An XTerra RP-C18 reverse phase column (4.6 x 250 mm, 5 μ m particle size) was used with an applied gradient elution method of 7-70% MeCN in 0.1M TEAA over 40 min. The conjugation reactions were found to proceed smoothly (52-87%) in the cases in which the antisense (A) linear RNA targeting GRP78 mRNA (Scheme 3, samples 1-5) was functionalized with saturated, unsaturated and polyunsaturated fatty acids. Similar reaction conversions (52-76%) were also observed for the palmitamide functionalized sense (S) linear RNA strands (Scheme 3, samples 6-8) targeting GRP75, GRP78 and GRP94 mRNA. Subsequently, the V-shape RNA template, targeting GRP78 and GRP94 mRNA as well as the Y-shape RNA targeting GRP 75, 78 and 94 were subjected to the same HCTU/DIEA coupling procedure for the incorporation of palmitic acid at the 5'-terminus (Scheme 3, samples 9-10). The conjugation reactions produced good conversions for the V-shape RNA bioconjugate (69 %) according to RP IP HPLC. However, little product (<5%) was detected with the Y-shape RNA template. The latter can be attributed to difficulties associated with conjugation reactions onto more complex and lengthier higher-order RNA templates.³⁴ In order to circumvent this limitation, an alternative strategy was developed in which palmitic acid was initially conjugated to the 5'-ends of the linear, complementary sense strands targeting GRP 75, 78 and 94 mRNA (Scheme 3, samples 6-8), followed by hybridization onto the RNA templates (Scheme 4). In this manner, linear, V- and Y-shape GRP targeting siRNAs containing single (i), double (ii) and triple (iii) palmitamides were self-assembled to directly improve transfection efficiency for more potent GRP knockdown and cell death in cancer cells.³¹

Scheme 4. Self-assembly of i. V- and ii. Y-shape multi-palmitamide labeled siRNA constructs.

FITC labeling of siRNAs

In a related study, the linear, V- and Y-shaped RNA templates targeting GRP-75, 78, and 94 mRNA were once more synthesized by automated solid-phase RNA synthesis following our previously reported procedure.¹⁸ Following RNA synthesis, a 5'-DMS(O)-MT-Amino C6 modifier (6-(4,4'-dimethoxy-4"-methylsulfonyl-tritylamino)hexyl- (2-cyanoethyl)-(N,N-diisopropyl)-

phosphoramidite, Glen Research Inc.) was coupled to the 5' end which, upon detritylation, produced a free amino group for bioconjugation with the reporter fluorophore, fluorescein isothiocyanate (FITC) following a previously reported procedure (Scheme 5).³²

Scheme 5. Solid phase bioconjugation of linear, V- and Y- shape FL-RNA bioconjugates.

The covalent attachment of FITC onto the support-bound RNA templates was achieved by reacting in the dark the fluorophore in 20% DMF in a 0.1 M carbonate-bicarbonate buffer (pH 8-8.5). The reaction was agitated on a shaker at room temperature (22 °C) for 48 h with the linear RNA template, while the V-shaped RNA required 72 h reaction and no product was observed with the Y-shape RNA template, even after a 3 day reaction period. The samples were subsequently handled in the dark, washed with water, DMF and MeCN until no orange color from any unreacted FITC remained visible in the supernatant. The support-bound fluorescein, FL-RNA samples were dried under Ar_(g) (5 min) and then transferred into autoclaved screw-cap microtubes and treated with a 1 mL solution of 3:1 v/v NH₄OH:EtOH at 55 °C for 16 to 20 h to complete sample cleavage from the support and deprotection of nucleobase and phosphate protecting groups. The supernatant was transferred to another autoclaved screw-cap microtube, evaporated to dryness in a Speed Vac concentrator and the CPG was washed twice with autoclaved distilled water (500 μL) to extract the RNA samples. Samples were then evaporated *in-vacuo* and re-suspended in a mixture of 1:1.5 v/v TEA-3HF:DMSO to complete the 2'-desilylation reaction at 65 °C for 2 h. The crude RNA samples were subsequently precipitated from the reaction mixture using 3 M NaOAc in n-BuOH. Precipitation was completed at low temperature (-80 °C) for 30 min prior to centrifugation (12,000 rpm) leaving the crude FL-labeled RNA samples as a solid yellowish-white pellet. The FL-labeled RNA samples were dried in a SpeedVac concentrator (Thermo Scientific) and dissolved in autoclaved water (1 mL) for yield determination using UV absorbance measurements at 260 and 488 nm.

The unique structures of the V- and Y-shaped RNA templates allowed for the incorporation of multiple fluorophores within the same molecular construct. This was achieved by labeling the complementary sense strands of the RNA templates, as previously described, followed by hybridization to the higher-order siRNAs with multiple fluorescent probes (Figure 4). The latter approach overcame the limitations associated with the direct conjugation of FITC with the Y-shape RNA template and provided the ability to generate GRP silencing siRNAs containing single (linear), double (V-shape) and triple (Y-shape) fluorescent probes for improving siRNA detection in cancer cells.³⁰

Figure 4. Rational design of GRP silencing i. linear, ii. V-shape and iii. Y-shape FL-siRNA bioconjugates.

The RNA templates were then purified by RP IP HPLC and their identities were confirmed by ESI MS. Purified FL-RNA templates were then quantitated by UV-Vis spectroscopy at 260 nm (UV) and the presence and quantity of fluorescein (and therefore the stoichiometry) was determined by monitoring absorption in the range 460-490 nm (Vis). The purified FL-RNA templates were subsequently hybridized with their complementary RNA strands, whereas, the unlabeled RNA templates were hybridized with their complementary FL-RNA sense strands in the annealing Tris buffer (10 mM Tris, 50 mM NaCl, 1 mM EDTA, pH 7.5 – 8.0) for structure-activity relationship studies.³⁰

CONCLUSIONS

The solid phase synthesis and self-assembly of higher order siRNAs and their bioconjugates provides an efficient method for improving siRNA activity in cells. Our work described an efficient methodology for building on solid support linear, V- and Y-shape RNA templates that self-assemble with their complementary RNA strands into higher-order siRNA motifs. These motifs have been shown

to adopt genetically encoded nanostructures, which also triggered potent RNAi activity in cancer cells. Moreover, bioconjugation with fatty acids and fluorescein enabled live tracking of siRNA activity in cancer cells without the need of an external transfection reagent. The latter provides the opportunity to develop potent siRNA theranostics that can be useful in the detection and treatment of cancer *in vitro* and *in vivo*. These applications are a current and long-term focus of our research objectives involving the development of efficient protocols that may enable the generation of new and improved gene therapeutics in the fight against cancer.

ACKNOWLEDGMENTS

The authors would like to thank the Department of Chemistry and Biochemistry at Seton Hall University for continued support. This research was gratefully supported by the University Research Council at Seton Hall University.

CONFLICT OF INTEREST

The authors have declared no conflicts of interest.

FIGURE LEGENDS

Figure 1. A) Design of a non-linear tripartite siRNA tripod based on the complementary base pairing of three independent siRNA sequences. B) Structural assembly of RNA and RNA-DNA “nanocubes” that could efficiently deliver up to six siRNA after Dicer cleavage. Adapted with permission from ref. 16, Afonin, K.A.; Viard, M.; Kagiampakis, I.; Case, C.L.; Dobrovolskaia, M.A.; Hofmann, J.; Vrzak, A.; Kireeva, M.; Kasprzak, W.K.; KewalRamani, V.N.; Shapiro, B.A. *ACS Nano* **2015**, 9(1), 251-259. Copyright 2015, American Chemical Society. C) Sequence dependent assembly of 3- and 4- way siRNA junctions. D) Design of V- and Y-shape siRNAs containing up to three siRNA sequences within the same molecular scaffold.

Figure 2. Representative examples of siRNA bioconjugates. A) lipid-siRNA bioconjugates. Figure adapted with permission from ref. 23, Kubo, T.; Yanagihara, K.; Sato, Y.; Nishimura, Y.; Kondo, S.; Seyama, T. *Bioconjugate Chem.* **2013**, 24(12), 2045-2057. Copyright 2013, American Chemical Society. B) Fluorescent-siRNA conjugated polymers used to image live cells. Figure adapted with permission from ref. 29, Liu, Y. Gunda, V.; Zhu, X.; Xu, X.; Wu, J.; Askhatova, D.; Farokhzad, O.C.; Parangi, S.; Shi, J. *Proc Natl Acad Sci U S A* **2016**, 113(28), 7750-7755. Copyright 2016, National Academy of Sciences. Higher order V and Y-shape siRNA construct demonstrating the ability to incorporate multiple C) lipid functionalities or D) fluorescent tags.

Scheme 1. Solution-phase synthesis of the ribouridine branchpoint phosphoramidites, **5**.

Scheme 2. Solid phase synthesis of linear, V-, Y- and >-< shape RNA.

Figure 3. Design and self-assembly of siRNA nanostructures. The RNA templates, namely, linear, V- and Y-shaped RNA were designed and synthesized according to our previously described methodology.¹⁸ The V- and Y-shaped templates incorporated a branchpoint ribouridine (rU) which allowed the incorporation of sense (S) and antisense (A) RNA. These templates preorganized the self-assembly of siRNA nanostructures which resembled circles, triangles, squares, rectangles, pentagons, hexagons and porous-type structures. These siRNA nanostructures targeted a single (1), double (1, 2) and triple (1, 2, 3) sites of oncogenic GRP-75, 78 and 94 mRNA. Figure adapted with permission from ref. 19, Patel, M.R.; Kozuch, S.D.; Cultrara, C.N.; Yadav, R.; Huang, S.; Samuni, U.; Koren, J., Chiosis, G.; Sabatino, D. *Nano Lett.* **2016**, *16*(10), 6099–6108. Copyright 2016, American Chemical Society.

Scheme 3. Solid-phase bioconjugation of the amino-linked linear, V and Y-shaped RNA templates with various fatty acids to afford the amide-linked fatty acid-RNA bioconjugates.

Scheme 4. Self-assembly of i. V- and ii. Y-shape multi-palmitamide labeled siRNA constructs.

Scheme 5. Solid phase bioconjugation of linear, V- and Y- shape FL-RNA bioconjugates.

Figure 4. Rational design of GRP silencing i. linear, ii. V-shape and iii. Y-shape FL-siRNA bioconjugates.

GTOC. The solid phase synthesis and self-assembly of higher-order siRNA motifs such as the GRP silencing linear, V-shape and Y-shape siRNAs and their bioconjugates have led to the development of new and improved gene therapeutics. In this method, a branchpoint ribouridine is used for the self-assembly of the multi-GRP silencing RNAs. Bioconjugation with bio-active probes (*e.g.* fatty acids and

This article is protected by copyright. All rights reserved.

fluorophores) enabled structure-function relationship studies in cancer cell models overexpressing GRP activity.

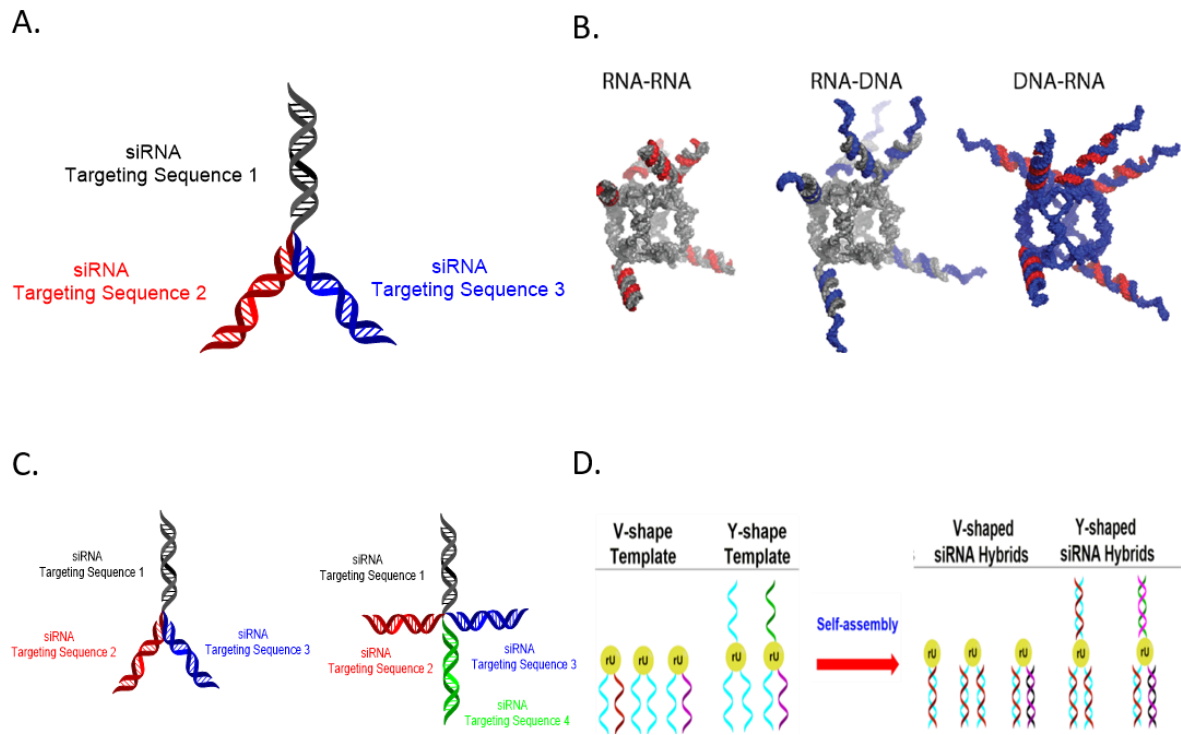
REFERENCES

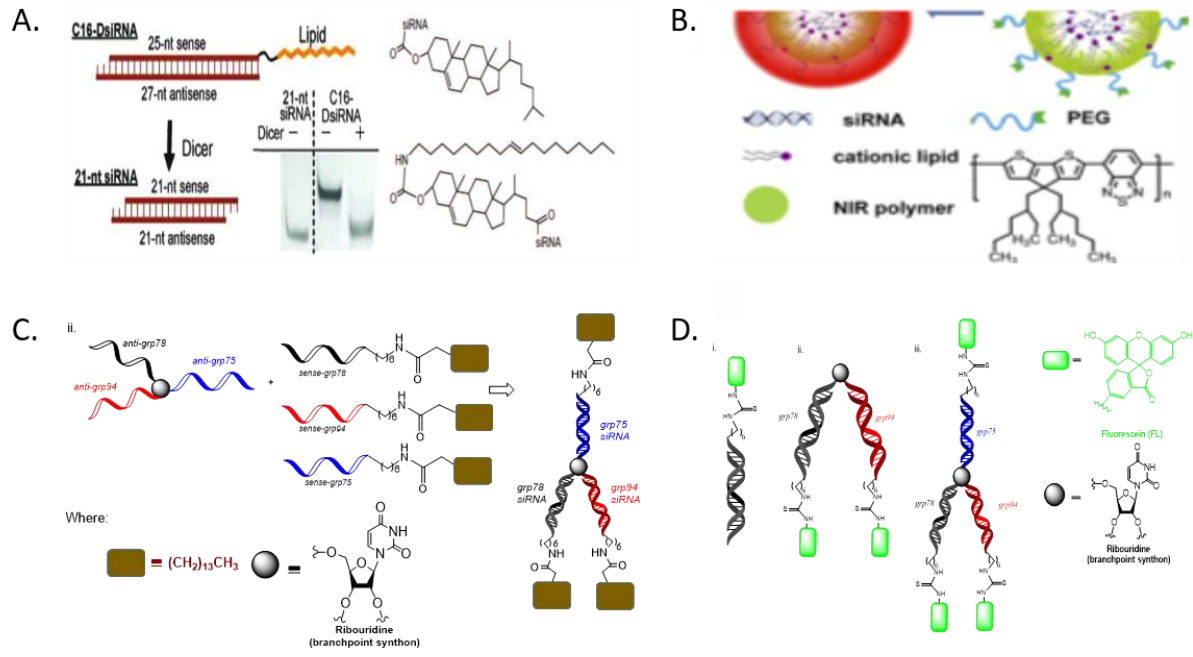
1. Ryther, R.C.C.; Flynt, A.S.; Phillips, J.A.; Patton, J.G. siRNA therapeutics: big potential from small RNAs. *Gene Therapy* **2005**, *12*(1), 5-11.
2. Shankar, P.; Manjunath, N.; Lierberman, J. The prospect of silencing disease using RNA interference *JAMA* **2005**, *293*(11), 1367-1373.
3. Titze-de-Almeida, R.; David, C.; Titze-de-Almeida, S.S. The Race of 10 Synthetic RNAi-Based Drugs to the Pharmaceutical Market. *Pharm. Res.* **2017**, *34*(7), 1339-1363.
4. Chiu, Y.L.; Rana, T.M. RNAi in human cells: Basic structural and functional features of small interfering RNA. *Mol. Cell* **2002**, *10*(3), 549-561.
5. Elbashir, S.M.; Harboth, J.; Lendeckel, W.; Yalcin, A.; Weber, K.; Tuschl, T. Duplexes of 21-nucleotide RNAs mediate RNA interference in cultured mammalian cells. *Nature* **2001**, *411*(6836), 494-498.
6. Kurreck, J. siRNA Efficiency: Structure or Sequence - That is the Question. *J Biomed Biotechnol* **2006**, *2006*(4), 83757.
7. MacRae, I.J.; Zhou, K.; Li, F.; Repic, A.; Brooks, A.N.; Cande, W.Z.; Adams, P.D.; Doudna, J.A. Structural basis for double-stranded RNA processing by Dicer. *Science* **2006**, *311*(5758), 195-198.
8. Zamore, P.D.; Tuschl, T.; Sharp, P.A.; Bartel, D.P. RNAi: Double-stranded RNA directs the ATP-dependent cleavage of mRNA at 21 to 23 nucleotided intervals. *Cell* **2000**, *101*(1), 25-33.
9. Chiu, Y.L.; Rana, T.M. siRNA function in RNAi: A chemical modification analysis. *RNA* **2003**, *9*(9), 1034-1048.
10. Lima, W.F.; Wu, H.; Nichols, J.G.; Sun, H.; Murray, H.M.; Crooke, S.T. Binding and cleavage specificities of human Argonaute2. *J Biol Chem.* **2009**, *284*(38), 26017-26028

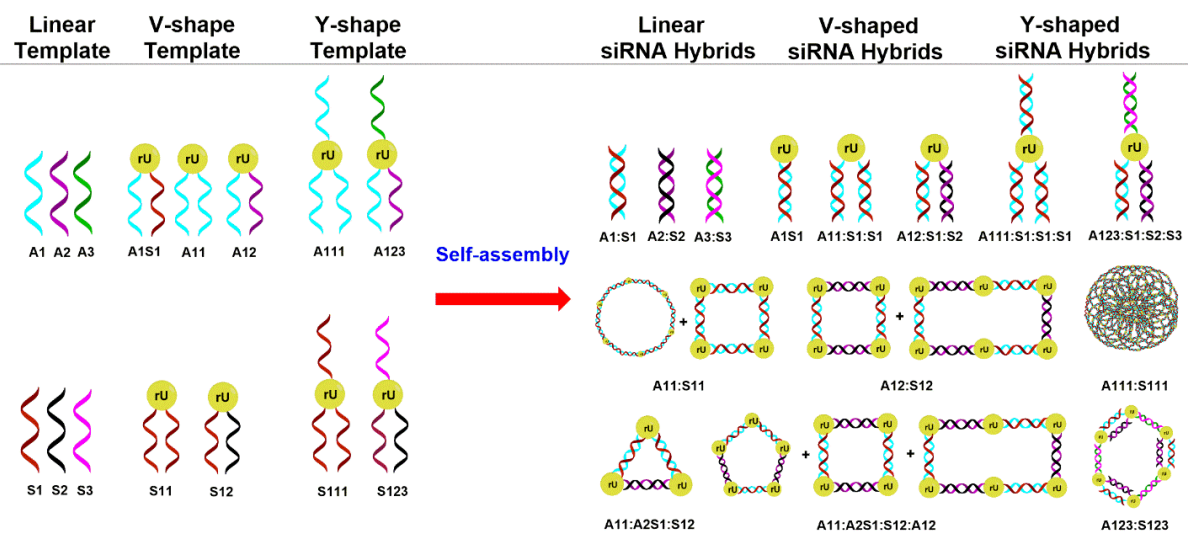
11. Bumcrot, D.; Manoharan, M.; Koteliensky, V.; Sah, D. W. RNAi therapeutics: a potential new class of pharmaceutical drugs. *Nature Chem Bio.* **2007**, *2*(12), 711-719.
12. Wang, S.; Shi, Z.; Liu, W.; Jules, J.; Feng, X. Development and validation of vectors containing multiple siRNA expression cassettes for maximizing the efficiency of gene silencing. *BMC Biotechnol.* **2006**, *6*, 50.
13. Sajeesh, S.; Lee, T.Y.; Kim, J.K.; Son, D.S.; Hong, S.W.; Kim, S.; Yun, W.S.; Kim, S.; Chang, C.; Li, C.; Lee, D.K. Efficient intracellular delivery and multiple-target gene silencing triggered by tripodal RNA based nanoparticles: a promising approach in liver-specific RNAi delivery. *J Control Release.* **2014**, *196*, 28-36.
14. Guo, P. The emerging field of RNA nanotechnology. *Nat Nanotechnol* **2010**, *5*(12), 833-842.
15. Shukla, G.C.; Haque, F.; Tor, Y.; Wilhelmsson, L. M.; Toulmé, J.J.; Isambert, H.; Guo, P.; Rossi, J.J.; Tenenbaum, S.A.; Shapiro, B.A. A boost for the emerging field of RNA nanotechnology. *ACS Nano* **2011**, *5*(5), 3405-3418.
16. Afonin, K.A.; Viard, M.; Kagiampakis, I.; Case, C.L.; Dobrovolskaia, M.A.; Hofmann, J.; Vrzak, A.; Kireeva, M.; Kasprzak, W.K.; KewalRamani, V.N.; Shapiro, B.A. Triggering of RNA interference with RNA-RNA, RNA-DNA, and DNA-RNA nanoparticles. *ACS Nano* **2015**, *9*(1), 251-259.
17. Nakashima, Y.; Abe, H.; Abe, N.; Aikawa, K.; Ito, Y.; Branched RNA nanostructures for RNA interference. *Chem Comm* **2011**, *47*(29), 8367-8369.
18. (a) Maina, A.; Blackman, B.A.; Parronchi, C.J.; Morozko, E.; Bender, M.E.; Blake, A.D.; Sabatino, D. Solid-phase synthesis, characterization and RNAi activity of branch and hyperbranch siRNAs. *Bioorg Med Chem Lett.* **2013**, *23*(19), 5270-5274., (b) Sabatino, D. Expanding the Sizes and Shapes of Nucleic Acids: Studies on Branched and Heptose Based Nucleic Acids. *Ph.D. Thesis*, McGill University, **2007**, 264pp.
19. Patel, M.R.; Kozuch, S.D.; Cultrara, C.N.; Yadav, R.; Huang, S.; Samuni, U.; Koren, J.; Chiosis, G.; Sabatino, D. RNAi Screening of the Glucose-Regulated Chaperones in Cancer with Self-Assembled siRNA Nanostructures. *Nano Lett.* **2016**, *16*(10), 6099–6108.

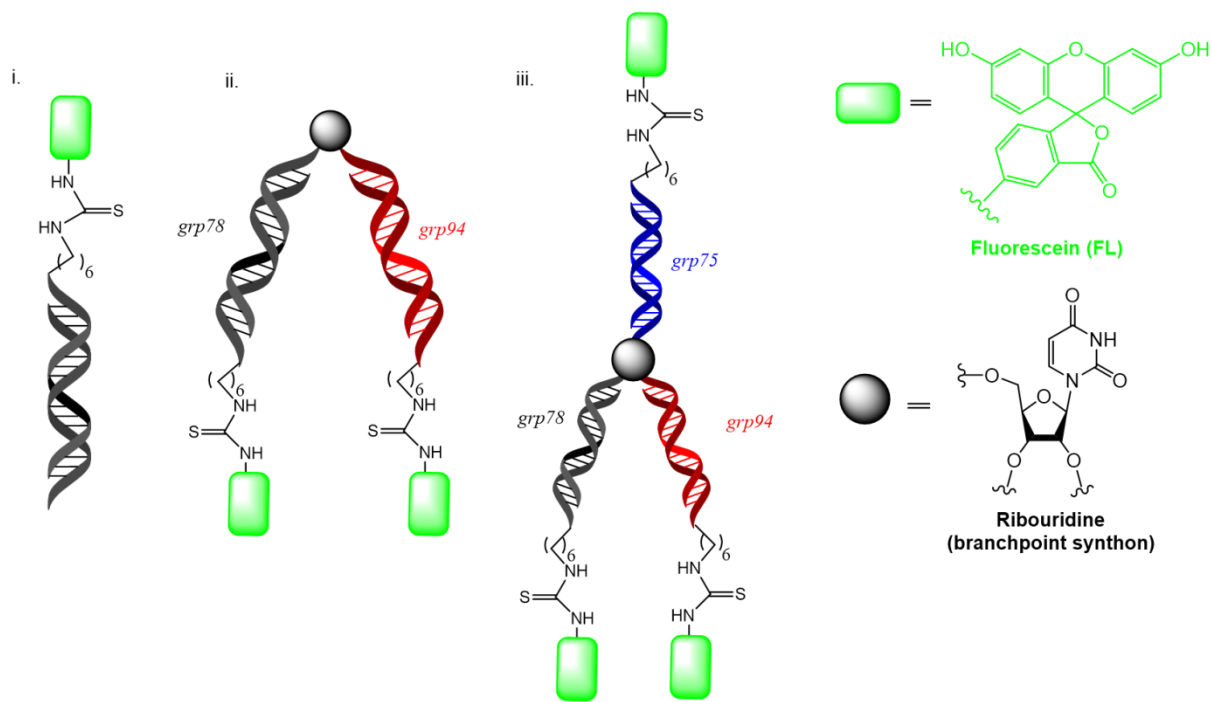
20. Zuckerman, J.E.; Gritl, I.; Tolcher, A.; Heidel, J.D.; Lim, D.; Morgan, R.; Chmielowski, B.; Ribas, A.; Davis, M.E.; Yen, Y. Correlating animal and human phase Ia/Ib clinical data with CALAA-01, a targeted, polymer-based nanoparticle containing siRNA. *Proc Natl Acad Sci U S A* **2014**, *111*(31), 11449-11454.
21. Patel, P.L.; Rana, N.K.; Patel, M.R.; Kozuch, S.D.; Sabatino, D. Nucleic Acid Bioconjugates in Cancer Detection and Therapy. *ChemMedChem* **2016**, *11*(3), 252-269.
22. Musacchio, T.; Vaze, O.; D'Souza, G.; Torchilin, V.P. Effective Stabilization and Delivery of siRNA: Reversible siRNA-Phospholipid Conjugate in Nanosized Mixed Polymeric Micelles. *Bioconjugate Chem.* **2010**, *21*(8), 1530-1536.
23. Kubo, T.; Yanagihara, K.; Sato, Y.; Nishimura, Y.; Kondo, S.; Seyama, T. Gene-Silencing Potency of Symmetric and Asymmetric Lipid-conjugated siRNAs and its Correlation with Dicer Recognition. *Bioconjugate Chem.* **2013**, *24*(12), 2045-2057.
24. Kubo, T.; Yanagihara, K.; Takei, Y.; Mihara, K.; Morita, Y.; Seyama, T. Palmitic Acid-Conjugated 21-Nucleotide siRNA enhances Gene-Silencing Activity. *Mol. Pharm.* **2011**, *8*(6), 2193-2203.
25. Kubo, T.; Takei, Y.; Mihara, K.; Yanagihara, K.; Seyama, T. Amino-Modified and Lipid-Conjugated Dicer-Substrate siRNA enhances RNAi Efficacy. *Bioconjugate Chem.* **2012**, *23*(2), 164-173.
26. Jeong, J.H.; Mok, H.; Oh, Y.K.; Park, T.G. siRNA conjugate delivery systems. *Bioconjugate Chem.* **2009**, *20*(1), 5-14.
27. Sumer, B.; Gao, J. Theranostic nanomedicine for cancer. *Nanomedicine* **2008**, *3*(2), 137-140.
28. Zhao, J.; Mi, Y.; Feng, S.S. siRNA-based nanomedicine. *Nanomedicine* **2013**, *8*(6), 859-862.
29. Liu, Y.; Gunda, V.; Zhu, X.; Xu, X.; Wu, J.; Askhatova, D.; Farokhzad, O.C.; Parangi, S.; Shi, J. Theranostic near-infrared fluorescent nanoplatform for imaging and systemic siRNA delivery to metastatic anaplastic thyroid cancer. *Proc Natl Acad Sci U S A* **2016**, *113*(28), 7750-7755.

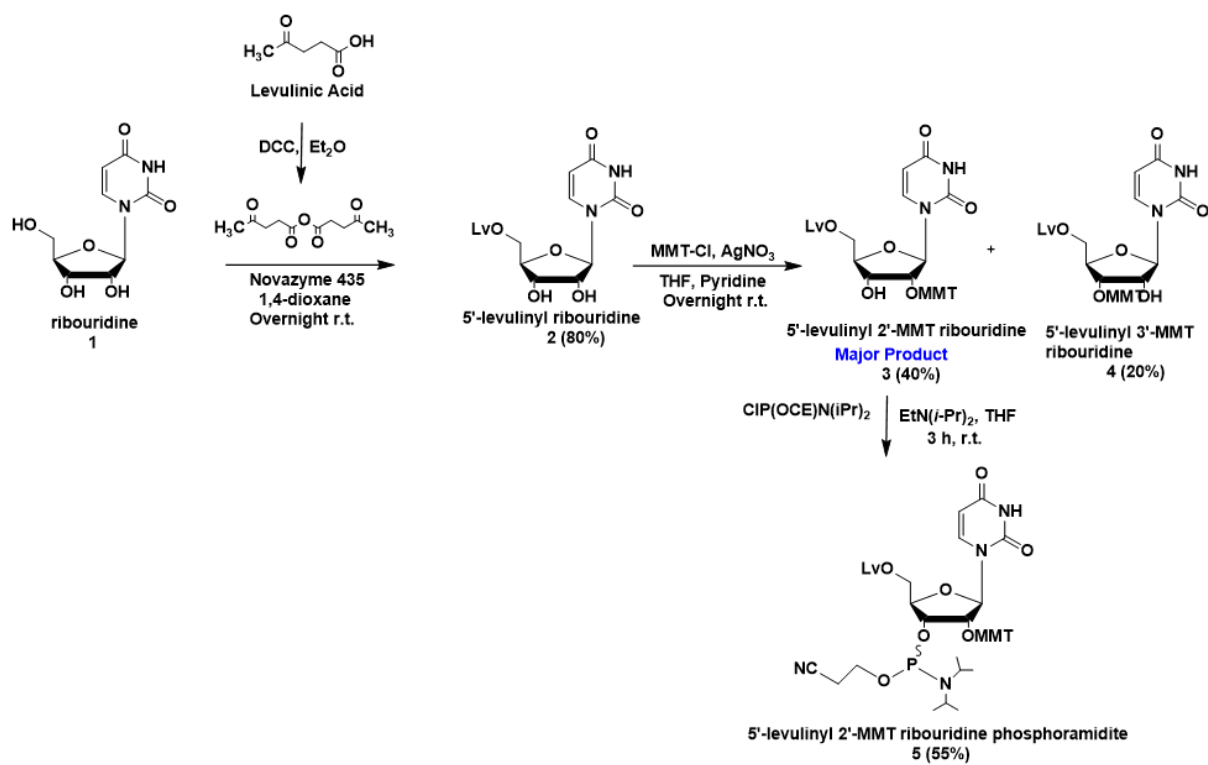
30. Kozuch, S.; Cultrara, C.; Beck, A.; Heller, C.; Shah, S.; Patel, M.; Zilberberg, J.; Sabatino, D. Enhanced cancer theranostics with self-assembled, multi-labeled siRNAs. *ACS Omega* **2018**, 3(10), 12975-12984.
31. Shah, S.; Cultrara, C.; Kozuch, S.; Patel, M.; Ramos, J.; Samuni, U.; Zilberberg, J.; Sabatino, D. Direct transfection of fatty acid conjugated siRNAs and the knockdown of the glucose regulated chaperones in prostate cancer cells. *Bioconjugate Chem.* **2018**, Article ASAP, doi: 10.1021/acs.bioconjchem.8b00580.
32. Murakami, A; Nakaura, M; Nakatsuji, Y; Nagahara, S; Tran-Cong, Q; Makino, K. Fluorescent-labeled oligonucleotide probes: detection of hybrid formation in solution by fluorescence polarization spectroscopy. *Nucleic Acids Res.* **1991**, 19(15), 4097-4102.
33. Liu, J.; Hennink, W.E.; van Steenbergen, M.J.; Zhuo, R.; Jiang, X. Versatile Supramolecular Gene Vector Based on Host-Guest Interaction. *Bioconjug Chem.* **2016**, 27(4), 1143-1152.
34. Kurschat, W.C.; Müller, J.; Wombacher, R.; Helm, M. Optimizing splinted ligation of highly structured small RNAs. *RNA.* **2005**, 11(12), 1909-1914.

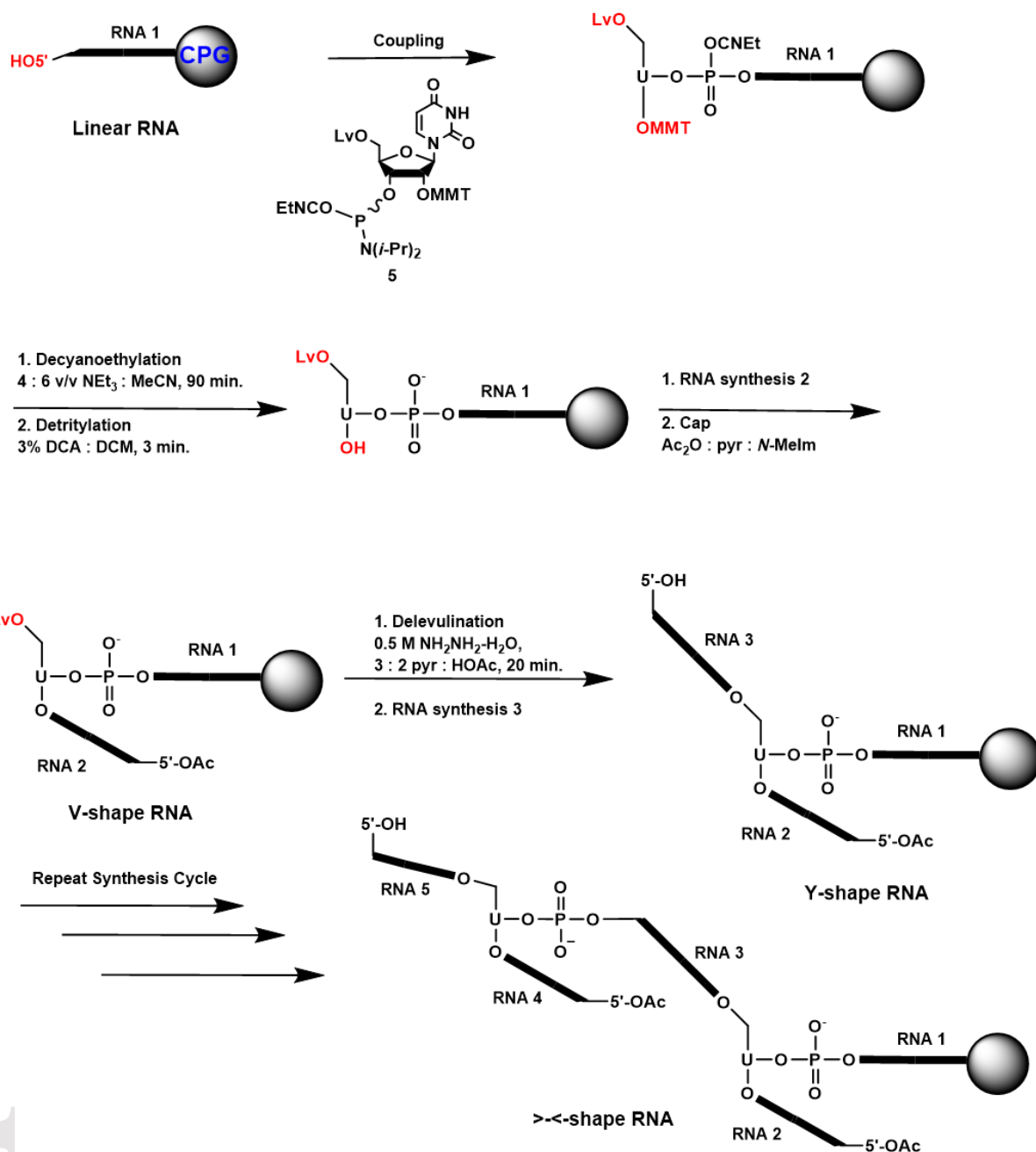


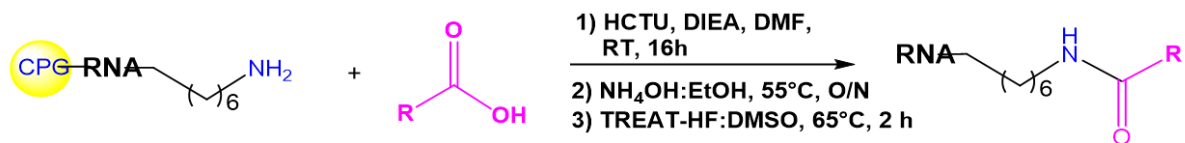


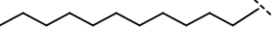
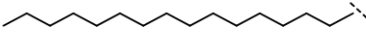
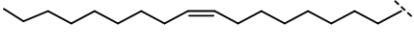
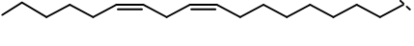
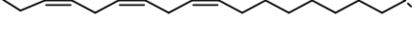




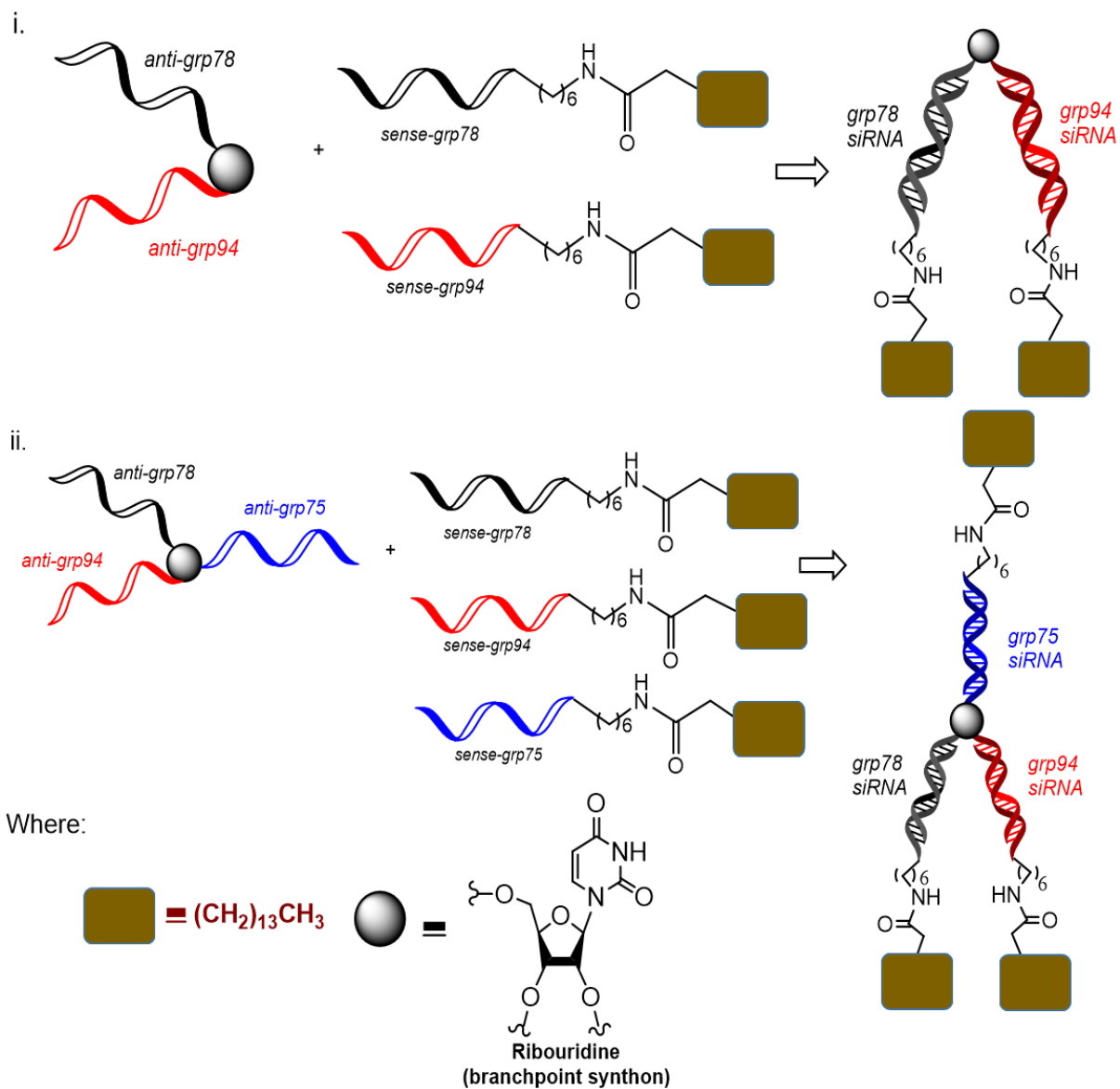


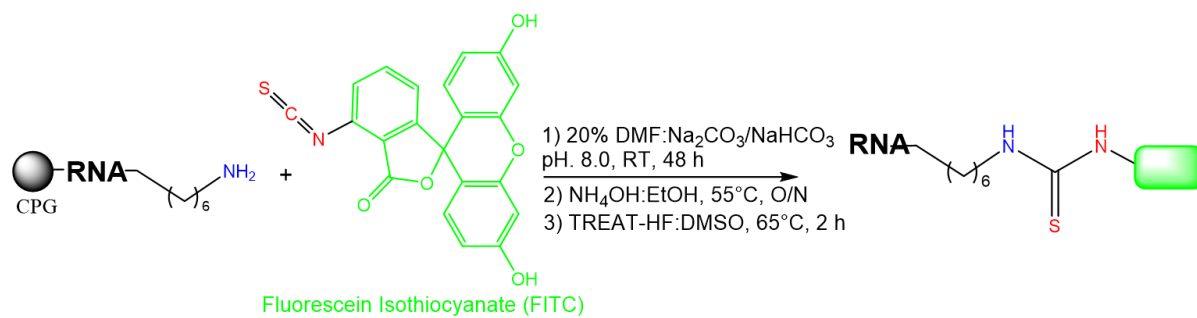




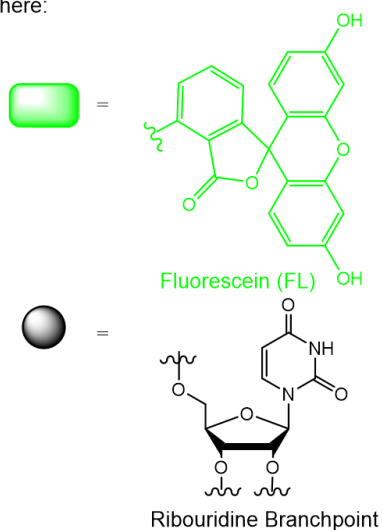
Sample #	RNA	R	% Conversions ^a
1)	 <i>grp78</i>		78 %
2)			86 %
3)			87 %
4)			52 %
5)			75 %
6)			65 %
7)	 <i>grp75</i>		76 %
8)	 <i>grp94</i>		52 %
9)	 <i>grp78</i>  <i>grp94</i>		69 %
10)	 <i>grp78</i>  <i>grp94</i>  <i>grp75</i>		<5 %

^aConversions based on RP IP HPLC analysis at 260 nm





Where:



RNA	% Conversion ^a
a) GRP78	58%
b) GRP78 GRP94	40%
c) GRP78 GRP94 GRP75	<5%

^aConversions based on RP IP HPLC analysis at 260 and 488 nm